

# Single-scattering by mineral dust particles modeled with spheroids

S. Merikallio<sup>\*1</sup>, H. Lindqvist<sup>2</sup>, T. Nousiainen<sup>2</sup>, and M. Kahnert<sup>3</sup>

<sup>1</sup>*Department of Climate Change, Finnish Meteorological Institute, P.O. box 503, FI-00101 Finland.*

<sup>2</sup>*Department of Physics, University of Helsinki, P.O. box 48, 00014 Finland.*

<sup>3</sup>*Swedish Meteorological and Hydrological Institute, Folkborgsvägen 1, S-60176 Sweden.*

We study how well different mineral dust samples can be modeled using spheroids and whether the best-fit spheroidal shape distributions bear any similarities that would allow us to suggest a generic first-guess shape distribution for dust. Overall, spheroids are found to fit the measurements significantly better than Mie spheres. However, it seems that best-fit shape distributions vary between samples and even between wavelengths considerably, making suggestions for a first-guess shape distribution difficult.

## INTRODUCTION

Mineral dust is a very abundant aerosol species in the Earth's atmosphere with a considerable and largely uncertain radiative impact. We are interested in using spheroids to model their radiative impact in a climate model where shape distribution information is not available; thus, finding a generic, accurate shape distribution would be desirable.

## MODELING APPROACH

We compare laboratory measurements [1, 2] with scattering matrices calculated from a dust optical database [3]. Measurements exist at wavelengths of 441.6 nm and 632.8 nm. The refractive indices ( $m$ ) of the samples are not known accurately so, for simulations, we try four different  $m$  with  $\text{Re}(m) = 1.55$  and  $1.7$ , and  $\text{Im}(m) = 0.001$  and  $0.01$ . The shapes include aspect ratios from 1.2 to 2.8 with an increment of 0.2 for both oblate and prolate spheroids. In addition, the special case of spheres is computed.

For comparisons with simulations, the measured  $F_{11}$  element needs to be properly normalized. To this end, the measurements are extrapolated using simulated values for scattering angles  $0 - 5^\circ$  and the value measured at  $173^\circ$  for angles of  $174 - 180^\circ$  so that the normalization integral can be applied.

The cost function for assessing the separation between measurements and model is calculated at the measurement points from  $5^\circ$  to  $170^\circ$  with steps of  $5^\circ$ , thus excluding  $171^\circ$ ,  $172^\circ$  and  $173^\circ$  to preserve the angular equality in error analysis.

---

\* Corresponding author: Sini Merikallio (Sini.Merikallio@fmi.fi)

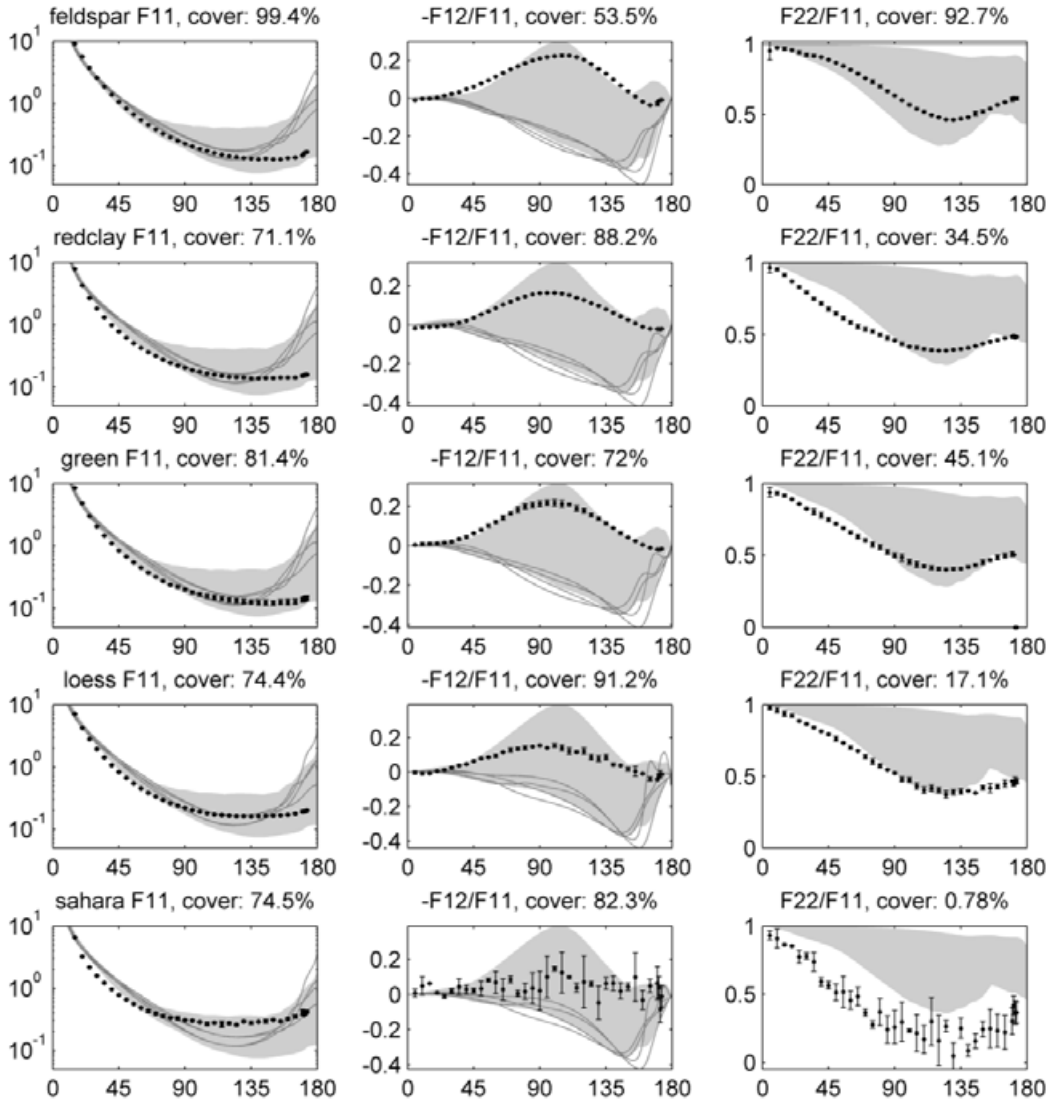


**Figure 1.** Coverages of measured scattering matrix elements by modeled spheroids at 632.8 nm wavelength for selected matrix elements. Each row corresponds to one sample from smallest (feldspar) to the largest effective radii (Sahara). Measurements are shown with diamonds and error bars, the shaded area indicates the coverage by all different spheroids (shapes and refractive indices) excluding spheres. The Mie spheres are shown with solid lines for each refractive index. Measured  $F_{11}$  elements have been normalized using the  $n = 3$  shape distribution by [4].

## ASSESSING THE OVERALL PERFORMANCE OF SPHEROIDS

The first task is to investigate how well the measured scattering matrix elements can be covered by spheroids of different shapes and refractive indices, since full coverage of measured matrix element by model spheroids is a necessary, but not sufficient, condition for fitting the measurements with simulations. In Fig. 1 three scattering matrix elements have been plotted for each dust sample studied for the wavelength of 632.8 nm. At each measurement point it is seen how much of the measurement error bar falls within the spheroid span, i.e. the relative amount of black dots that fall within the shaded area, and finally averages of these percents are tabulated and shown in subtitles. We believe the poor coverage of the depolarization element  $F_{22}$  is caused by smooth-surfaced spheroids being unable to mimic the scattering response of real rough-surfaced particles. This discrepancy is stronger for larger particles.

The coverage percentages averaged over all matrix elements and for the  $F_{11}$  element separately are shown in Table 1 for both wavelengths. It can be seen that, overall, the measurements for the samples with smallest particles can be better covered by spheroids than those for the larger ones. Interestingly, loess is covered remarkably well for its size, even comparably to the red clay.

**Table 1.** Coverages of spheroids for different particles.

	$r_{\text{eff}}$ ( $\mu\text{m}$ )	441.6 nm, %			632.8 nm, %		
		$F_{11}$	avg.	std.	$F_{11}$	avg.	std.
feldspar	1.0	100	<b>92</b>	5	99	<b>89</b>	19
red clay	1.5	72	<b>62</b>	24	71	<b>58</b>	24
green clay	1.55	84	<b>61</b>	29	82	<b>63</b>	19
loess	3.9	76	<b>55</b>	35	75	<b>59</b>	27
Sahara	8.2	23	<b>43</b>	34	75	<b>48</b>	29

## BEST-FIT SHAPE DISTRIBUTIONS

The suitability of shape distribution parameterization developed by [4] in simulating the mineral dust optical properties is investigated. Optimal shape distributions for spheroids are sought by varying the exponent  $n$  of the parametrized shape distribution, computing a cost function for the goodness of agreement, and finding the optimal value for  $n$ . In addition, we carry out fitting exercises using a non-linear fitting algorithm for selected cases. The latter method is much more demanding, but allows us to find shape distributions where the weight for each shape is optimal and independent from each other. As the fitting method can return other kinds of shape distributions than the  $n$  parametrized shape distribution, it also works as an assessment for the applicability of the first method.

Table 2 summarizes the results for the optimal parametrized shape distributions under different criteria. As the cost functions, we consider  $\chi^2$  error for the phase function  $F_{11}$ , average  $\chi^2$  error for the size independent non-zero phase matrix elements, error below which 80% of points fall (D80), again for both  $F_{11}$  and averaged over independent non-zero phase matrix elements, and finally the asymmetry parameter ( $g$ ) difference.

Obviously, best fits are obtained at different  $n$  for different cases. Interestingly, they are often obtained either with the smallest (0) or largest (18)  $n$  considered. The  $F_{11}$  element, often

the most important, however, is uniformly best modeled with the equiprobable distribution ( $n=0$ ). Curiously, unlike  $F_{11}$ , the asymmetry parameter  $g$  is best reached with values of  $n$  larger than zero. This may be because the calculation of asymmetry parameter takes into account also the diffraction peak whilst the other criteria only consider angles between  $5^\circ$  and  $170^\circ$ . One intermediate value of refractive index, namely  $m = 1.6 + 0.003i$  is currently being added into our analysis.

From table 2 we see that each row contains multiple refractive indices, implying that inversion of the refractive index from spheroidal simulations is not very robust for mineral dust and may be subject to artifacts arising from the use of simplified model shapes.

**Table 2.** The best-fit  $n$  values of shape distributions [4] using different criteria. The refractive index with which the best-fit value was obtained is indicated by: a =  $1.55 + 0.001i$ ; b =  $1.55 + 0.01i$ ; c =  $1.7 + 0.001i$ ; and d =  $1.7 + 0.01i$ .

	441.6 nm					632.8 nm				
	$F_{11}$	avg.	D80 $F_{11}$	D80 avg.	$g$	$F_{11}$	avg.	D80 $F_{11}$	D80 avg.	$g$
Feldspar	0 b	3 a	0 ab	0/1 ab	2 a	0 b	2 b	0 c	0 c	9 a
red clay	0 b	18 c	0 a	0 d	1 a	0 b	18 d	0 a	0 d	3 b
green clay	0 b	18 d	0 c	0 c	1 b	0 b	18 d	0 c	1 c	3 b
Loess	0 d	18 c	0 a	0 d	4 c	0 a	0 a	0 b	0 b	18 d
Sahara	0 c	0 c	0 b	0 b	0 c	0 c	0 c	0 b	0 d	0 d

While the spheroidal scheme is superior to that of spheres, its performance is far from perfect especially for samples with larger particles. The optimal shape distributions seem to vary from sample to sample, and also between wavelengths. This suggests the optimal spheroidal shape distribution is not connected to the shapes of the dust particles.

## REFERENCES

- [1] H. Volten, O. Muñoz, E. Rol, J. F. de Haan, W. Vassen, J. W. Hovenier, K. Muinonen, and T. Nousiainen. Scattering matrices of mineral aerosol particles at 441.6 nm and 632.8 nm. *JGR* **106**(D15) (2001).
- [2] O. Muñoz, H. Volten, J. F. e Haan, W. Vassen, and J. W. Hovenier. Experimental determination of scattering matrices of randomly oriented fly ash and clay particles at 442 and 633 nm. *JGR* **106**(D19) (2001).
- [3] O. Dubovik, A. Sinyuk, T. Lapyonok, B. N. Holben, M. Mishchenko, P. Yang, T. F. Eck, H. Volten, O. Muñoz, B. Veihelmann, W. J. van der Zande, J-F. Leon, M. Sorokin, and I. Slutsker. Application of spheroid models to account for aerosol particle nonsphericity in remote sensing of desert dust. *JGR* **111**(D11208) (2006).
- [4] T. Nousiainen, M. Kahnert, and B. Veihelmann. Light scattering modeling of small feldspar aerosol particles using polyhedral prisms and spheroids. *JQSRT* **101** (2006).